JVI Journals.ASM.org

Modified Vaccinia Virus Ankara-Based Vaccine Vectors Induce Apoptosis in Dendritic Cells Draining from the Skin via both the Extrinsic and Intrinsic Caspase Pathways, Preventing Efficient Antigen Presentation

E. Guzman,[a] C. Cubillos-Zapata,[a] M. G. Cottingham,[b] S. C. Gilbert,[b] H. Prentice,[a] B. Charleston,[a] and J. C. Hope[a]*

Institute for Animal Health, Compton, Newbury, Berkshire, United Kingdom,[a] and The Jenner Institute, Oxford University, Oxford, United Kingdom[b]

Dendritic cells (DC) are potent antigen-presenting cells and central to the induction of immune responses following infection or vaccination. The collection of DC migrating from peripheral tissues by cannulation of the afferent lymphatic vessels provides DC which can be used directly *ex vivo* without extensive *in vitro* manipulations. We have previously used bovine migrating DC to show that recombinant human adenovirus 5 vectors efficiently transduce afferent lymph migrating DEC-205$^+$ CD11c$^+$ CD8$^-$ DC (ALDC). We have also shown that recombinant modified vaccinia virus Ankara (MVA) infects ALDC *in vitro*, causing downregulation of costimulatory molecules, apoptosis, and cell death. We now show that in the bovine system, modified vaccinia virus Ankara-induced apoptosis in DC draining from the skin occurs soon after virus binding via the caspase 8 pathway and is not associated with viral gene expression. We also show that after virus entry, the caspase 9 pathway cascade is initiated. The magnitude of T cell responses to mycobacterial antigen 85A (Ag85A) expressed by recombinant MVA-infected ALDC is increased by blocking caspase-induced apoptosis. Apoptotic bodies generated by recombinant MVA (rMVA)-Ag85A-infected ALDC and containing Ag85A were phagocytosed by noninfected migrating ALDC expressing SIRPα via actin-dependent phagocytosis, and these ALDC in turn presented antigen. However, the addition of fresh ALDC to MVA-infected cultures did not improve on the magnitude of the T cell responses; in contrast, these noninfected DC showed downregulation of major histocompatibility complex class II (MHC-II), CD40, CD80, and CD86. We also observed that MVA-infected ALDC promoted migration of DEC-205$^+$ SIRPα$^+$ CD21$^+$ DC as well as CD4$^+$ and CD8$^+$ T cells independently of caspase activation. These *in vitro* studies show that induction of apoptosis in DC by MVA vectors is detrimental to the subsequent induction of T cell responses.

Modified vaccinia virus Ankara (MVA) was derived from *Vaccinia virus* through more than 500 blind passages *in vitro* in chicken embryo fibroblasts (CEF) (50). This resulted in vaccinia virus losing about 15% of its genome. With the exception of the Syrian hamster cell line BHK-21, the ability of MVA to replicate in most mammalian primary cells and cell lines has been lost, although genome replication, late-gene expression, and immature virion formation are still able to occur, except in human blood-derived dendritic cells (DC), in which only early viral genes are expressed (7, 20). This makes MVA an attractive candidate for its use as a vaccine vector to deliver recombinant proteins and induce protective immunity. Recombinant MVA (rMVA) has been used in various preclinical and phase I and phase II clinical trials against a number of infectious agents or tumor-associated antigens (10, 19, 45, 55, 56).

DC are potent antigen-presenting cells capable of priming naïve T lymphocytes and are central to the induction of immune responses following infection or vaccination. Most systems used to investigate DC-T cell interactions rely on the isolation of monocytes or macrophages from blood or tissues (such as spleen or bone marrow) (63, 71), followed by maturation with interleukin 4 (IL-4) and granulocyte-macrophage colony-stimulating factor (GM-CSF) or the harvesting of tissues followed by isolation of resident DC. Only the model of cannulation of lymphatic vessels provides biological material, including DC derived from anatomical sites used in vaccination (31, 32, 34, 49, 68). Various DC models have been used to identify MVA-DC interactions to try to understand rMVA-induced immunogenicity. Murine bone marrow-derived DC (BMDC) showed high levels of apoptosis following infection with MVA *in vitro* but were still capable of inducing antigen-specific T cell responses when these cells were transferred to naïve mice (2). Another study showed that these MVA-infected BMDC were phagocytosed by uninfected DC (47); however, antigen presentation by the latter was not demonstrated. More recently, mouse BMDC were used to demonstrate an adjuvant capacity of MVA itself even in the presence of virus-induced apoptosis (58). In the human system, MVA has also been shown to induce apoptosis in monocyte-derived DC (moDC) (11, 43). MVA was shown to stimulate moDC as a result of infection or using supernatants from HeLa cells infected with MVA (21) despite increased apoptosis. In agreement with data from the murine system, human uninfected DC have been shown to take up antigens from MVA-infected leukocytes (24). MVA-infected moDC also showed impaired migration toward the lymphoid chemokines CCL19 and CXCL12 (41) without affecting surface expression of the respective chemokine receptors.

Received 1 February 2012 **Accepted** 5 March 2012

Published ahead of print 14 March 2012

Address correspondence to E. Guzman, efrain.guzman@iah.ac.uk.

* Present address: The Roslin Institute, University of Edinburgh, Easter Bush, Midlothian, United Kingdom.

doi:10.1128/JVI.00264-12

Tuberculosis is a highly infectious disease caused in humans by *Mycobacterium tuberculosis*. Bovine tuberculosis is caused by *Mycobacterium bovis*, which is closely related to *M. tuberculosis*. *M. bovis* infections pose a risk to human health and are also a major economic problem in both the developing and the developed world. *M. bovis* strain Bacille Calmette-Guerin (BCG) does not protect against adult pulmonary tuberculosis, but it does show protection against disease when administered in both human and bovine neonates (13, 37). Antigen 85A (Ag85A) is a highly conserved mycobacterial protein present in all mycobacterial species. It has been shown to be immunodominant in both humans and animals, and viral vectors, including MVA, expressing Ag85A have been shown to increase immunogenicity when used in combination with BCG (54, 76).

In vivo targeting of dendritic cells by vaccines is an attractive approach for improving vaccination strategies (12). However, the study of vaccine-DC interactions *ex vivo* is limited by the availability of the relevant dendritic cells, that is, DC draining from the head mucosae in intranasal vaccinations protocols and DC draining from the skin in subcutaneous/intradermal/intramuscular vaccinations approaches. Afferent lymphatic DC (ALDC) represent a major population of migrating DC (14, 16, 28, 81) with functional and phenotypic heterogeneity. We and others have described ALDC as being high forward scatter (FSC^{high}) DEC-205^+ $CD11c^+$ $CD8^-$ (17, 28, 34); within this population, subpopulations expressing various levels of SIRPα (CD172a), CD11a, CD26, and CD13 have also been described (5, 28, 29, 40). These populations have been shown to interact with and stimulate T cells differently and have differential cytokine secretion profiles (35, 40, 52, 72). A detailed understanding of *in vivo* populations of DC at relevant anatomical sites is important to vaccine design.

We have recently described the differential effects of viral vectors on bovine dendritic cells draining from the skin (17). We reported that, similar to murine BMDC and human moDC, MVA induces apoptosis in DC draining from the skin. We now report the kinetic analysis of MVA-induced apoptosis in ALDC, and in contrast to what was observed for BMDC or moDC, this occurs within the first few hours after infection. We also provide evidence of the induction of both the intrinsic and the extrinsic pathways of caspase-induced apoptosis. By blocking MVA-induced caspase activity, we were able to increase antigen presentation to both $CD4^+$ and $CD8^+$ T cells. We also provide evidence that apoptotic bodies that are generated by rMVA infection, and that contain the recombinant protein of interest, are phagocytosed by noninfected ALDC expressing SIRPα via an actin-mediated mechanism and that these cells in turn present phagocytosed antigen to T cells. However, the addition of fresh ALDC to MVA-infected cultures did not increase the magnitude of the T cell responses; in contrast, these noninfected DC showed downregulation of major histocompatibility complex class II (MHC-II), CD40, CD80, and CD86. We also observed that MVA-infected ALDC promote migration of DEC-205^+ SIRPα$^+$ $CD21^+$ DC as well as $CD4^+$ and $CD8^+$ T cells independently of caspase activation. Our model is relevant in two ways: first, we are using dendritic cells draining from the skin with minimal manipulation and so these are relevant in intramuscular/intradermal/subcutaneous vaccination protocols; second, we are using an animal model relevant to the disease since cattle are a host species for mycobacterial infection. These data provide a mechanistic description of recombinant-MVA induced immunity using dendritic cells obtained from anatomically relevant sites.

MATERIALS AND METHODS

Pseudoafferent lymphatic cannulation. MHC-defined, conventionally reared 6-month-old Friesian Holstein calves (*Bos taurus*) from the Institute for Animal Health (IAH) herd were used for these studies. Cannulations were performed essentially as previously described (34). Lymph was collected into sterile plastic bottles containing heparin (10 U/ml), penicillin, and streptomycin. The lymph collected was either used fresh or centrifuged (300 × *g* for 8 min) and resuspended in fetal calf serum (FCS)-10% dimethyl sulfoxide (DMSO), and the cells were stored in liquid nitrogen prior to use. Mononuclear cells were isolated from the afferent lymph by density gradient centrifugation over Histopaque 1083 (Sigma). Ag85A-specific T cells were obtained from MHC-defined cattle vaccinated subcutaneously with 10^6 CFU of BCG Pasteur. All T cells used were collected at 3 weeks postvaccination at the peak of the response. All animal experiments were approved by the IAH ethics committee according to national United Kingdom guidelines.

MAb and flow cytometry. Fluorochrome-labeled mouse anti-bovine monoclonal antibodies (MAb) used in this study have been described in detail previously (5, 38–40, 66). These were CC98-allophycocyanin (APC) (anti-DEC-205), CC21-phycoerythrin (PE) (anti-CD21), CC14-PE (anti-CD1b), and CC149-peridinin chlorophyll protein (PerCP)/Cy5.5 (anti-SIRPα), ILA-16–Alexa Fluor 680/PE (anti-CD11c), ILA-21–PE (anti-MHC-II), ILA-88–fluorescein isothiocyanate (FITC) (anti-MHC-I), ILA-156–PE (anti-CD40), N32/52-3–PE (anti-CD80) ILA-159–PE (anti-CD86), CC30-APC/Cy5.5 (anti-CD4), CC63-APC/Cy7 (anti-CD8), ILA-111–Alexa Fluor 610/PE (anti-CD25), and CC302-PE (anti-gamma interferon [anti-IFN-γ]). Control MAb were isotype- and concentration-matched anti-avian MAb (34, 80). Dead cells were gated out using the 405-nm excitable dye LIVE/DEAD Aqua or propidium iodide (PI; Invitrogen) in accordance with the manufacturer's instructions. The cells were analyzed using an LSRFortessa (Becton Dickinson), and staining was assessed using FCS Express version 3 (DeNovo Software). Afferent lymph DC were distinguished from other cells on the basis of their high forward scatter (FSC^{high}) and high-intensity expression of DEC-205 (28, 34). Only live single events were used for analysis.

Cell sorting. Cells were sorted into dendritic cell subpopulations by use of a FACSAria II cell sorter (Becton Dickinson) and purities confirmed by flow cytometry using FACSDiva version 5 (Becton Dickinson). T cell subsets were magnetically separated using monoclonal antibody cell sorting (MACS) technology (Miltenyi Biotech, Germany) in accordance with the manufacturer's instructions. Typically, the purity of the resulting dendritic and T cell subsets was over 97% as determined by flow cytometry.

Recombinant vectors. The generation of recombinant MVA expressing mycobacterial antigen 85A (Ag85A) has been described previously (54). Recombinant replication-deficient human adenovirus 5 (Ad5) expressing Ag85A was generated as described previously (53). rMVA and recombinant adenovirus 5 (rAd5) expressing green fluorescent protein (GFP) were used as negative controls. Vectors were produced by the Jenner Institute Viral Vector Core Facility University of Oxford, United Kingdom.

UV inactivation of recombinant MVA. To inactivate viral DNA replication, recombinant MVA-Ag85A stocks were treated with 1 μg/ml of Psoralen (Calbiochem) and irradiated in a Stratalinker 1800 UV crosslinker (Stratagene) with a 365 nm UV lamp following the method described previously (74).

Mycobacterial antigens. Purified protein derivative from *M. bovis* (PPD-B) was obtained from the tuberculin production unit at the Veterinary Laboratories Agency (VLA), Weybridge, United Kingdom, and was used at 10 μg/ml. Recombinant antigen 85A (Ag85A) was obtained from Lionex GmbH (Germany) and used at 2 μg/ml in all assays.

Infection of afferent lymph cells. Afferent lymph cells were cultured in tissue culture medium (TCM; Iscove's modified Dulbecco's medium [IMDM] containing 10% FCS [Autogen Bioclear, United Kingdom], 10^{-5} M 2-β-mercaptoethanol [Sigma-Aldrich, Poole, United Kingdom]), with the recombinant viruses using optimal multiplicities of infection (MOI) described previously (17).

Apoptosis assays. Cells were resuspended to 1×10^6 cells per 0.1 ml in annexin V staining buffer (apoptosis kit; R&D Systems, Minneapolis, MN) and stained with annexin V-Pacific Blue and propidium iodide or LIVE/DEAD Aqua (Invitrogen) in accordance with the manufacturer's instructions and analyzed by flow cytometry.

Western blot analysis. To detect Ag85A expression in rMVA-infected ALDC or phagocytosed apoptotic bodies, flow-sorted cells were lysed in cell lysis buffer containing 0.5% NP-40, 50 mM $NaCl_2$, 20 mM Tris-HCl (pH 7.5). Fifty microliters of cell lysate was then mixed with equal volumes of sodium dodecyl sulfate (SDS)-polyacrylamide gel electrophoresis loading buffer (50 mmol/liter Tris-Cl [pH 6.8], 100 mmol/liter dithiothreitol, 2% sodium dodecyl sulfate, 0.1% bromophenol blue, and 10% glycerol) and denatured by boiling for 5 min. Samples were separated on a 12% sodium dodecyl sulfate-polyacrylamide gel, transferred to a nitrocellulose membrane, blocked with a 2% dry milk solution, and probed with either mouse anti-Ag85A monoclonal antibody clone TD-17 at a concentration of 2 μg/ml (a kind gift from K. Huygen, Pasteur Institute, Brussels, Belgium) or mouse anti-β-actin (Abcam). After extensive washing with phosphate-buffered saline (PBS) containing 0.5% Tween 20 (PBS-T), the membrane was incubated with a rabbit anti-mouse horseradish peroxidase-conjugated secondary antibody (Dako) at a final concentration of 5 μg/ml. After extensive washing with PBS-T, Ag85A was detected by luminescence using ECL Advance (Amersham) and autoradiography films (Amersham Hyperfilm ECL) were exposed for 1 min.

Inhibition of caspases. Specific and pan-specific caspase inhibitors were obtained from Merck Biosciences (Darmstadt, Germany) and used in accordance with the manufacturer's instructions. Caspase 3 inhibitor II Z-DEV-FMK, caspase 8 inhibitor II Z-IETD-FMK, caspase 9 inhibitor I Z-LEHD-FMK, and general caspase inhibitor Z-VAD-FMK were used at a 1 nM final concentration in accordance with the manufacturer's instructions. The negative control Z-FA-FMV and a DMSO control were used in all inhibition assays.

Caspase activity ELISA. ALDC (1×10^6) were infected with rMVA-Ag85A using an MOI of 3 PFU/cell and lysed after various infectious periods using lysis buffer containing 0.5% NP-40, 50 mM $NaCl_2$, 0.1% SDS in PBS. Caspase activity was then measured using either the caspase 8 or the caspase 9 activity enzyme-linked immunosorbent assay (ELISA; R&D Systems) in accordance with the manufacturer's instructions in 98-well flat-bottomed plates (Costar). A_{550} was measured using a FLUOstar Optima microplate reader (BMG Labtech, Germany).

Phagocytosis assays. Fluorescence-activated cell sorting (FACS)-sorted DC were labeled with the green-fluorescing dye PKH-67 (Sigma, United Kingdom) in accordance with the manufacturer's instructions. DC were then infected with rMVA-Ag85A using an MOI of 3 PFU/cell for 60 min at 37°C. The cells were washed twice with PBS, resuspended in TCM, and cultured overnight in 12-well plates (Costar). The following day, autologous FACS-sorted DC were labeled with the red-fluorescing dye PKH-46 (Sigma, United Kingdom) and added to MVA-infected cells at a ratio of 1:1. Cocultures were then incubated at 37°C or 4°C for 4 h to allow phagocytosis to occur, harvested, and analyzed by flow cytometry.

Inhibition of phagocytosis. To identify the mechanism of phagocytosis of rMVA-induced apoptotic bodies by ALDC, phagocytosis assays were set up as described above in the presence of the following inhibitors, which have been shown to block phagocytosis: cytochalasin D (10 μM; actin dependent [65]), fillipin (5 μg/ml; caveolae dependent [64]), chlorprozamine (10 μg/ml; prevents clathrin-coated-pit formation [78]), methyl-β-cyclodextrin (10 mM; cholesterol dependent [75]), and amiloride (10 mM; blocks Na^+ [79] and therefore macropinocytosis [66]). DMSO was used as a diluent control, and PBS was used as a negative control. All chemicals were obtained through Sigma-Aldrich (Poole, United Kingdom).

Confocal microscopy. FACS-sorted DC (FSC^{high} DEC-205^+) either freshly isolated or harvested from a phagocytosis assay were cultured on collagen-treated coverslips (Sigma) for 6 h to allow adhesion of cells to the coverslips. The cells were fixed with acetone at −20°C for 3 min, washed twice with PBS, permeabilized with 3% paraformaldehyde for 20 min, washed twice with PBS, and stained with DAPI (4′,6-diamidino-2-phenylindole; Invitrogen) in accordance with the manufacturer's instructions. Cells were mounted onto microscope slides using VectaShield (Vector Laboratories, United Kingdom) and observed using a Leica SP5 confocal microscope.

Migration assays. All assays were performed in triplicate. Three hundred microliters of culture supernatants from an overnight infection of ALDC with MVA-Ag85A was added to a 24-well plate (Corning), followed by addition of 8-μm Transwell inserts (Corning). ALDC (1×10^5) in a 100-μl total volume were then added to the inside compartment of the Transwell insert and incubated for 4 h at 37°C. The cells that migrated toward the lower compartment were harvested and analyzed by flow cytometry. Migration index was calculated as the mean number of cells migrating toward the medium from MVA-infected DC divided by the mean number of cells migrating toward the medium from noninfected DC.

Antigen presentation and T cell responses. Populations of dendritic cells were FACS purified, washed five times with PBS, and incubated with recombinant vectors, recombinant Ag85A, PPD-B, or TCM for 90 min at 37°C in a 96-well U-bottomed plate (Costar). The cells were washed twice with PBS, resuspended in TCM, and mixed with either peripheral blood mononuclear cells (PBMC) or MACS-sorted $CD4^+$ T and $CD8^+$ T cells from MHC-matched BCG-vaccinated animals at a ratio of 1 DC to 10 T cells in a final volume of 200 μl (48). For detection of IFN-γ expression by an enzyme-linked immunospot (ELISPOT) assay, the cells were transferred to nitrocellulose-backed 96-well MultiScreen hemagglutinin (HA) plates (Millipore, Bedford, MA) which had been coated with 100 μl of 8 μg/ml anti-bovine IFN-γ MAb CC330. The cells were incubated for 24 h at 37°C, and the assay continued as previously described (36). In some assays, proliferation was assessed by labeling cells with carboxyfluorescein diacetate succinimydyl ester (CFDA-SE) as previously described (17). The results are shown as percent proliferation, determined as the percentage of $CFSE^{LOW}$ cells.

Statistical analyses. Data are presented as means ± standard deviations, and groups were compared using one-way analysis of variance (ANOVA) and pairwise comparison. Geographical and descriptive statistics as well as line and bar graphs were generated using GraphPad Prism version 5.04 for PC.

RESULTS

MVA-expressed Ag85A is not efficiently presented by ALDC. Since poxvirus-based vaccines are normally delivered by intradermal or subcutaneous administration or by scarification of the skin, the model of cannulation of pseudoafferent lymphatic vessels is relevant in providing biological material for *in vitro* studies of cells migrating from the skin toward lymph nodes. To test the hypothesis that antigens expressed by recombinant vectors are efficiently presented by afferent lymph dendritic cells (ALDC), we infected ALDC *in vitro* with recombinant MVA (rMVA) or recombinant adenovirus 5 (rAd5) expressing mycobacterial antigen 85A (Ag85A) or loaded cells with recombinant Ag85A or PPD-B to stimulate T cells from BCG-vaccinated animals. We have previously shown that by infecting ALDC with MVA-GFP at an MOI of 1 to 5 PFU/cell, the number of GFP^+ cells is similar to that of Ad5-GFP infected ALDC at an MOI of 100 IU/cell (17). We therefore used rMVA-Ag85A at an MOI of 3 PFU/cell and rAd5-Ag85A at 100 IU/cell. ALDC effectively stimulated IFN-γ secretion from

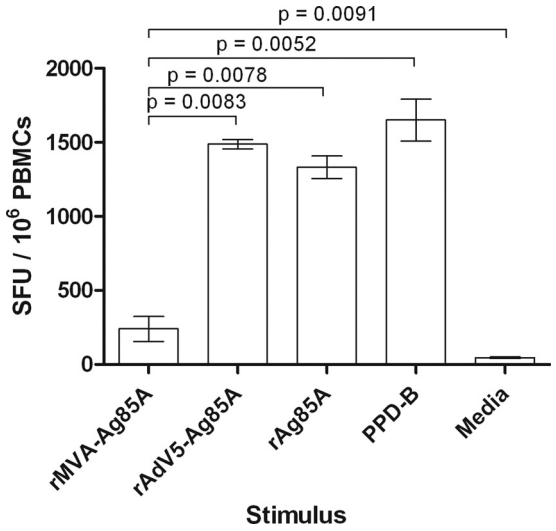

FIG 1 MVA-expressed Ag85A is not efficiently presented by ALDC. FACS-sorted FSC^{high} DEC-205$^+$ cells from MHC-defined animals were infected with recombinant viruses expressing Ag85A or loaded with rAg85A (2 μg/ml) or PPD-B (20 μg/ml) and were used as antigen-presenting cells. IFN-γ responses by PBMC from MHC-matched animals ($n = 8$) were measured by ELISPOT assay. Bars represent mean numbers of spot-forming units (SFU) per million PBMC. Error bars represent standard deviations of results from triplicate wells.

T lymphocytes following pulsing with rAg85A or PPD-B or when transduced with rAd5-Ag85A. Although ALDC infected with rMVA-Ag85A induced antigen-specific IFN-γ secretion higher than rMVA expressing GFP ($P = 0.0093$; data not shown) or cells cultured with medium alone ($P = 0.0091$), these levels were significantly lower than those for rAd5-Ag85A ($P = 0.0083$), rAg85A ($P = 0.0078$), and PPD-B ($P = 0.0052$) (Fig. 1).

ALDC become apoptotic 30 min after infection with recombinant MVA. Upon microscopic analysis of MVA-infected ALDC, the cells appeared rounded with membrane blebbing, indicative of apoptosis (data not shown). To confirm that MVA-infected ALDC became apoptotic, we infected freshly isolated ALDC with MVA at an MOI of 3 and stained the cells using annexin V and LIVE/DEAD stain before analysis by flow cytometry at various time points (Fig. 2). As early as 30 min postinfection, 20% of ALDC were annexin V positive (Fig. 2B), and at 24 h postinfection, over 50% of the cells were LIVE/DEAD positive, indicating significant levels of cell death (Fig. 2E). Samples cultured with UV-inactivated virus showed an initial increase in number of annexin V$^+$ cells, but this frequency remained constant (Fig. 2E). To confirm that the effect of cell death was due to virus infection, ALDC were infected with rMVA expressing GFP or with recombinant vector which had been UV inactivated. Compared to the level for mock-infected ALDC (Fig. 2F), Fig. 2G shows that the majority of LIVE/DEAD$^+$ cells were GFP$^+$, and Fig. 2H shows that GFP expression and cell death can be blocked by UV inactivation.

Both the intrinsic and the extrinsic caspase pathways are involved in MVA-induced apoptosis of ALDC. Apoptosis can be activated via two independent caspase pathways, the extrinsic pathway characterized by the activation of caspase 8 and the intrinsic pathway characterized by the activation of caspase 9. To identify if infection by rMVA induced caspase-mediated apoptosis, we infected ALDC with rMVA-A85A or UV-inactivated rMVA-Ag85A and collected cells at various time points. Caspase 8 and caspase 9 activities were measured by ELISA (Fig. 3). Caspase 8 activity was detected in ALDC infected with rMVA-Ag85A as soon as 2 h following infection and was significantly ($P = 0.0021$) higher than the level for the mock-infected control (Fig. 3A). At that time point, similar caspase 8 activity in ALDC infected with UV-inactivated virus ($P = 0.8951$) was measured. At 6 hours postinfection, caspase 8 activity in cells treated with both rMVA and UV-inactivated rMVA was not significant ($P = 0.6201$) compared to the level for mock-infected cells (Fig. 3A). In contrast, increased caspase 9 activity was not significant until 12 h postinfection ($P = 0.0039$) in ALDC infected with rMVA-Ag85A (Fig. 3B). Caspase 9 activity in cells cultured with UV-inactivated virus remained similar to that observed in uninfected cells ($P = 0.1089$).

ALDC were then infected with rMVA-Ag85A in the presence of apoptosis inhibitors. Preliminary results showed that by using a caspase 3 inhibitor or a nonspecific caspase inhibitor cocktail, the frequency of MVA-induced apoptosis was reduced (data not shown) compared to the level for the caspase inhibitor negative control. We therefore used a caspase 8 inhibitor to block the extrinsic pathway and a caspase 9 inhibitor to block the intrinsic pathway.

When ALDC were infected in the presence of a caspase 8 inhibitor, MVA-induced apoptosis was delayed compared to that in cells infected in the absence of caspase inhibitors (Fig. 3C), with significant differences observed at 2 ($P = 0.0402$) and 4 ($P = 0.0033$) h postinfection. No significant differences in apoptosis between MVA-infected ALDC in the presence or absence of caspase inhibitors ($P = 0.1256$) were observed at 6 h postinfection or later (Fig. 3C). In contrast, ALDC infected with MVA in the presence of caspase 9 inhibitor rapidly became apoptotic and died, and there were no significant differences between cells in the presence or absence of caspase 9 inhibitors at these early time points ($P = 0.5303$). At 6 h postinfection, the frequency of annexin V$^+$ ALDC infected with MVA in the presence of caspase 9 inhibitor was significantly different ($P = 0.0247$) from that of MVA-infected ALDC in the absence of caspase inhibitors. There was a reduction in the number of annexin V$^+$ cells in the later sample because these cells became annexin V$^-$ PI$^+$. To confirm that both caspase pathways were involved in MVA-induced apoptosis, we infected ALDC with rMVA in the presence of both caspase 8 and caspase 9 inhibitors. The combination of both inhibitors delayed the expression of annexin V for 12 h in MVA-infected cells compared to that in cells infected in the absence of inhibitors ($P = 0.0174$), and at 24 h postinfection, the use of inhibitors did not have an effect on the number of annexin V$^+$ cells ($P = 0.1741$) (Fig. 3E).

Blocking MVA-induced caspases in ALDC improves antigen presentation. To test the hypothesis that preventing or delaying MVA-induced apoptosis improves antigen presentation, ALDC collected from animals of known MHC haplotypes were infected with rMVA-Ag85A in the presence or absence of caspase inhibitors and these were then used to stimulate T cells from MHC-matched BCG-vaccinated animals. Following infection with rMVA-Ag85A, ALDC were able to induce a low frequency of expression of IFN-γ that was significantly lower than that induced by ALDC transduced with Ad5-85A or PPD-B as shown previously (Fig. 1). However, the addition of caspase inhibitors during MVA infection significantly increased ($P = 0.0058$) the capacity to induce secretion of IFN-γ by PBMC compared to the level for cells

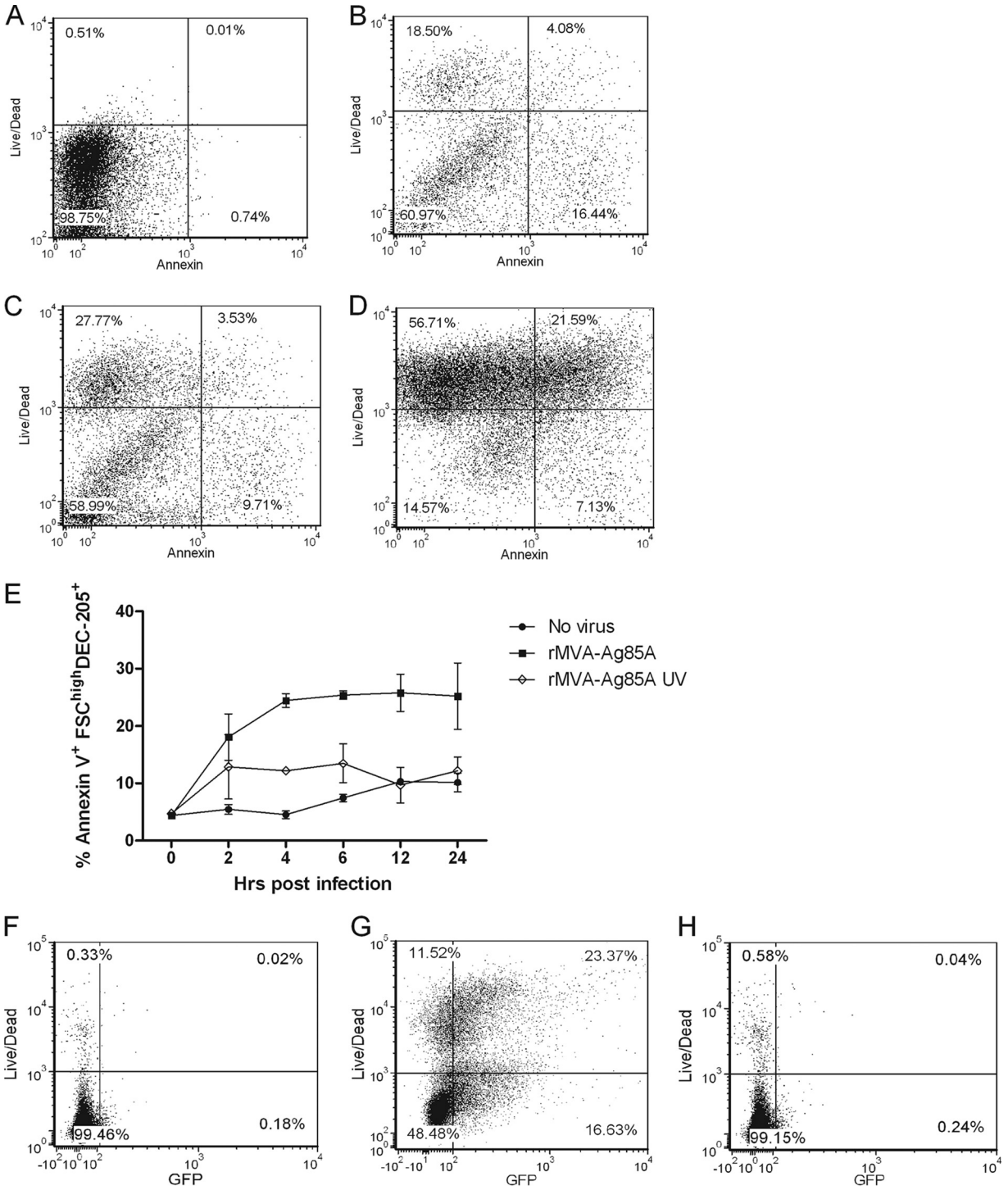

FIG 2 rMVA induces apoptosis in ALDC shortly after infection. ALDC were infected with rMVA-Ag85A or UV-inactivated virus at 4°C for 60 min to allow virus attachment; excess virus was removed by extensive washing, and cells were cultured at 37°C. Aliquots were then harvested at various time points, and apoptosis was measured using annexin V and LIVE/DEAD stain by flow cytometry. (A to D) Annexin V-LIVE/DEAD dot plots showing apoptosis before infection and at 30 min, 2 h, and 24 h postinfection within gated DEC205^{hi} ALDC. (E) Line graph showing the frequency of apoptotic ALDC after rMVA infection (black squares) compared with UV-inactivated rMVA (white diamonds) and mock-infected cells (black circles). Points indicate means of results from cells from 5 individual animals analyzed in duplicate, and error bars indicate standard deviations. (F to H) Dot plots showing GFP expression in MVA-infected cells. ALDC were mock infected (F) or infected with rMVA-GFP (G) or with UV-inactivated rMVA-GFP (H) as described above. Cell death and GFP expression in gated DEC205^{hi} ALDC were measured after 6 h by flow cytometry. Plots are representative of five individual experiments.

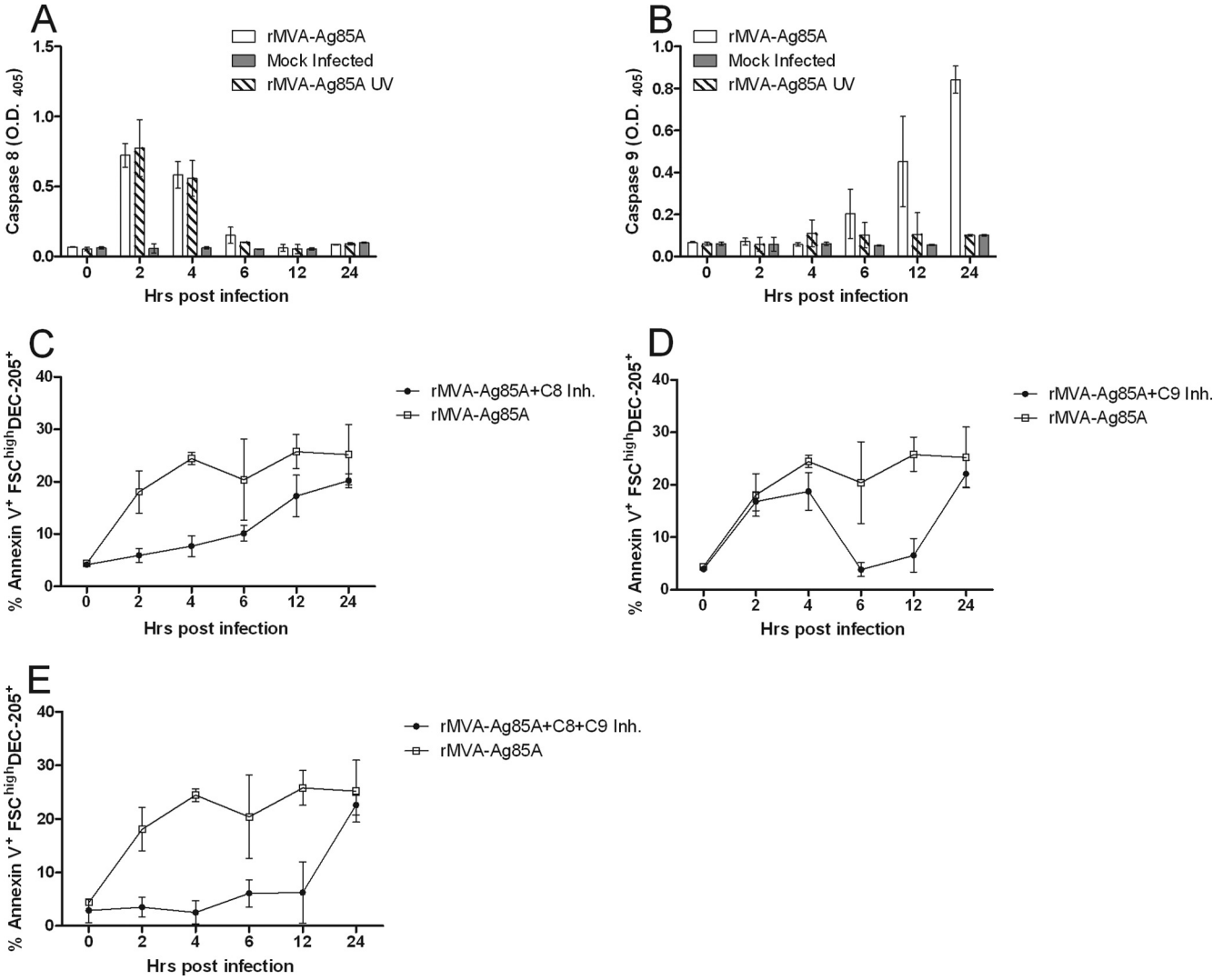

FIG 3 Both the extrinsic and the intrinsic caspase pathways are involved in apoptosis in MVA-infected ALDC. (A and B) ALDC (1×10^6) were infected with rMVA-Ag85A or UV-inactivated rMVA-Ag85A (MOI = 3) at 4°C for 60 min to allow virus attachment; excess virus was removed by extensive washing, and cells were cultured at 37°C. Aliquots were collected at various time points and cell lysates tested for caspase 8 (A) and caspase 9 (B) activity by ELISA. (C to E) ALDC (1×10^6) were infected with rMVA-Ag85A (MOI = 3) as described above in the presence of caspase 8 inhibitor (C), caspase 9 inhibitor (D), or both (E). Graphs represent means of results from cells from 5 different animals analyzed in duplicate. Error bars indicate standard deviations.

cultured in the absence of caspase inhibitors (Fig. 4A). The number of antigen-specific spot-forming units (SFU) in those samples containing rMVA plus inhibitors increased such that these samples were comparable to samples containing rAd5-Ag85 ($P = 0.5021$) and PPD-B ($P = 0.2913$). We also assessed the stimulation of T lymphocyte proliferation (Fig. 4B and C). Low-level stimulation of $CD4^+$ and $CD8^+$ proliferation was observed when ALDC were infected with MVA-Ag85A compared to the level for ALDC transduced with Ad5-Ag85A ($P = 0.0051$ and $P = 0.0041$ for $CD4^+$ and $CD8^+$, respectively) or pulsed with PPD-B ($P = 0.0017$ and $P = 0.0011$, respectively). However, significantly enhanced stimulation was observed when ALDC were infected with MVA-Ag85A in the presence of caspase inhibitors such that these responses were comparable to those for rAd5-Ag85A ($P = 0.8323$) and PPD-B ($P = 0.8979$). To confirm that apoptosis inhibitors did not have a nonspecific effect on antigen presentation, we measured Ag85A-specific IFN-γ release responses by ELISPOT assay using ALDC infected with rMVA-Ag85A, transduced with rAd5-Ag85A, or loaded with rAg85A, all in the presence or absence of inhibitors as antigen-presenting cells. Figure 4D shows that treatment with caspase inhibitors has a significant effect ($P = 0.0058$) in antigen presentation only in those samples infected with rMVA. Ag85A-specific responses obtained using rMVA-GFP were similar to those in mock-infected cells (data not shown).

Apoptotic bodies derived from MVA-infected ALDC are phagocytosed by noninfected ALDC. We demonstrated that MVA induced apoptosis and cell death in ALDC rapidly after infection *in vitro* and that this significantly hindered direct antigen presentation. However, MVA has been shown to be an effective vaccine vector especially in prime-boost vaccination protocols. In light of this dichotomy, we investigated potential mechanisms for antigen presentation. MVA-infected ALDC were labeled with PKH-67 (to label cellular membranes green) and cultured overnight, inducing apoptosis. Uninfected PKH-46 (red)-labeled

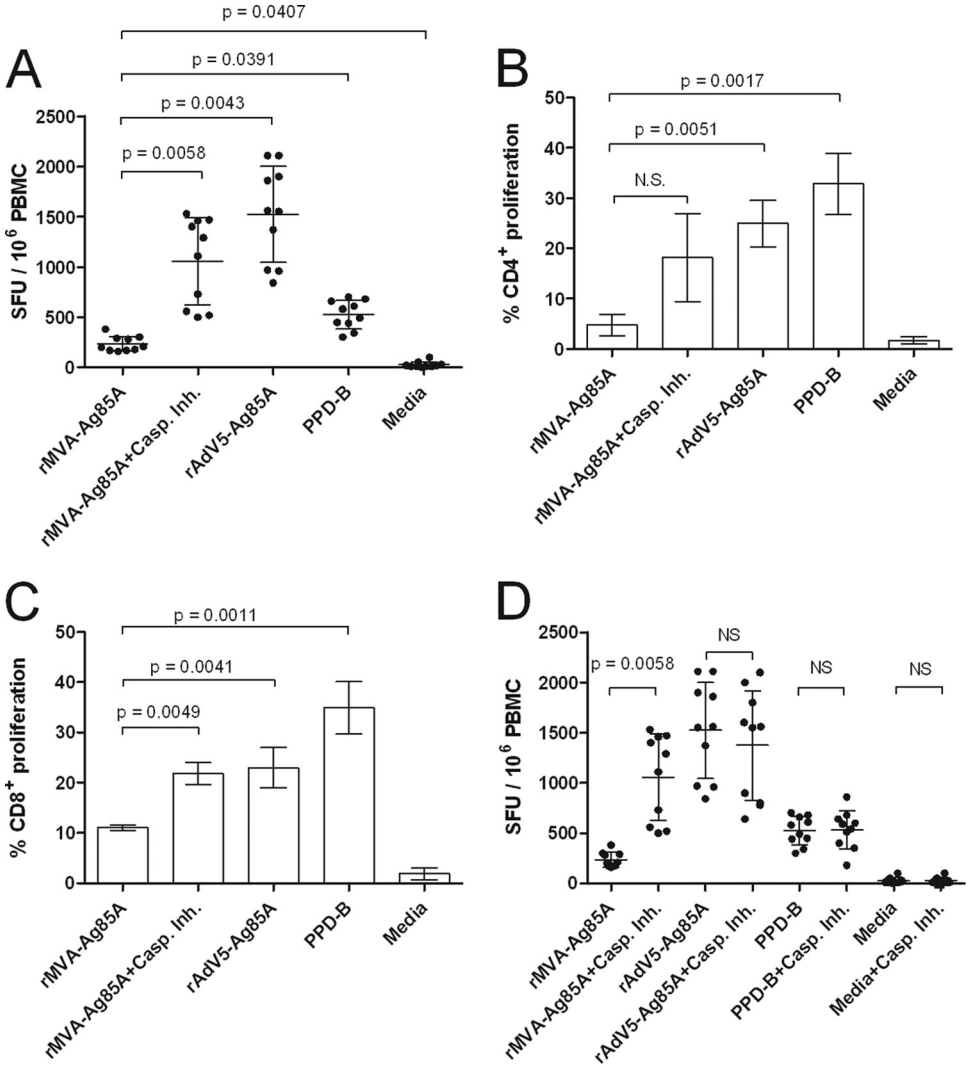

FIG 4 Blocking MVA-induced apoptosis improves antigen presentation *in vitro*. ALDC were infected with rMVA-Ag85A in the presence or absence of caspase inhibitor cocktail or with rAd5-Ag85A (as described in Materials and Methods), were loaded with mycobacterial PPD-B (20 μg/ml), or were mock infected. PBMC from MHC-matched BCG-vaccinated cattle ($n = 10$) were then added to ALDC cultures. IFN-γ responses were measured by ELISPOT assay (A and D), and $CD4^+$ (B) or $CD8^+$ (C) T cell proliferation was measured by CFDA-SE dilution by flow cytometry. Error bars indicate standard deviations of results from samples tested in duplicate.

ALDC were then added and cocultured with MVA-infected cells for 4 h at 37°C or 4°C prior to fluorescence measurement by flow cytometry (Fig. 5). Both MVA-infected and control ALDC were efficiently labeled (Fig. 5A and B). Coculture of MVA infected ALDC with uninfected ALDC at 37°C resulted in a significant number (~20%) of double-red-green-positive cells (Fig. 5D), indicating uptake of apoptotic cells by the uninfected ALDC. At 4°C, fewer than 10% of ALDC became double positive (Fig. 5C). To gain further insight, we FACS purified the three populations represented in Fig. 5D and detected Ag85A-containing cells by Western blot analysis (Fig. 5E). ALDC infected with rMVA-Ag85A expressed the Ag85A (lower right) and, following coculture rAg85A, was also expressed in ALDC that were not exposed directly to MVA-Ag85A (upper right), confirming that the uninfected ALDC have taken up material from the MVA-infected cells. We also analyzed the double-positive (upper right) population by confocal microscopy (Fig. 6). Apoptotic bodies from MVA-infected ALDC (green dots) were found within noninfected ALDC.

To identify the mechanism by which apoptotic bodies were taken up by ALDC, phagocytosis inhibitors were added to the cultures (Fig. 7A). The frequency of apoptotic body uptake by ALDC as described above was significantly reduced in the presence of cytochalasin D ($P = 0.0337$), indicating that this process was actin mediated. However, no significant differences were observed with other inhibitors (chlorprozamine [clarthin dependent], fillipin [caveolae dependent], amiloride [Na^+ channel blocker], and methyl-β-cyclodextrin [cholesterol dependent]).

We determined whether DC which had taken up antigen-containing apoptotic bodies from MVA-infected DC could present Ag85A to T lymphocytes making the recombinant antigen available within a nonapoptotic DC for cross-presentation. We infected ALDC with rMVA-Ag85A at an MOI of 3 and after an

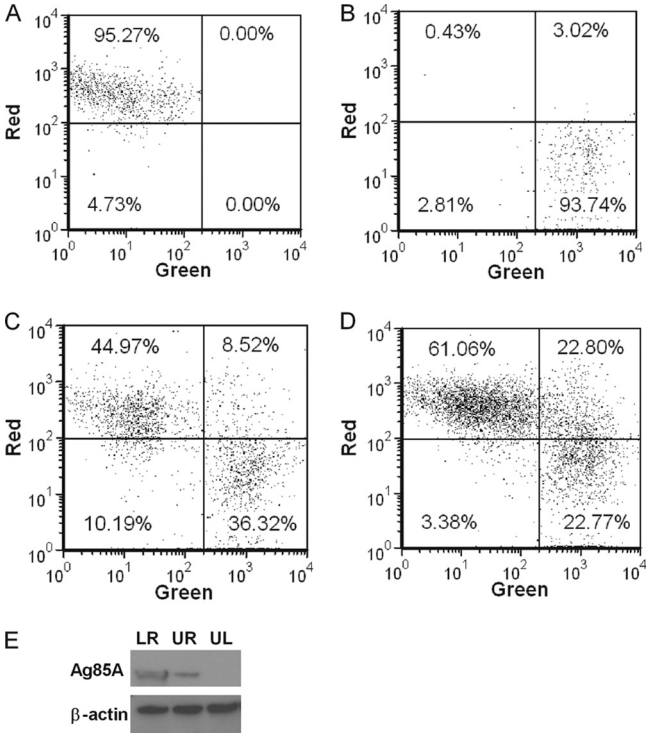

FIG 5 Apoptotic bodies from MVA-infected cells are phagocytized by noninfected DC. PKH-67-labeled ALDC were infected with rMVA-Ag85A (MOI = 3) as described in Materials and Methods and cultured overnight at 37°C. PKH-46-labeled autologous ALDC were then added to the culture, incubated at either 4°C or 37°C for 4 h, and analyzed by flow cytometry. (A) PKH-46-labeled (red) cells. (B) PKH-67-labeled (green) cells. (C) Mixed culture incubated at 4°C. (D) Mixed culture incubated at 37°C. Dot plots shown are gated on FSC^{high} $MHCII^+$ $CD11c^+$ $DEC205^+$ live single events and are representative of experiments performed using cells from 10 individual animals. (E) Western blot (representative of 3 independent experiments) showing the presence of Ag85A and β-actin in FACS-sorted ALDC from panel D. LR, lower right; UR, upper right; and UL, upper left.

overnight culture added an equal number of freshly isolated autologous ALDC and MHC-matched T cells. Phagocytosis inhibitors or controls were also added. ALDC which had taken up apoptotic bodies were able to present antigen and stimulate IFN-γ secretion (Fig. 7B); this was significantly reduced ($P = 0.0042$) in the presence of cytochalasin D (Fig. 7B). Similarly, ALDC were able to promote proliferation of $CD4^+$ (Fig. 7C) and $CD8^+$ T cells (Fig. 7D), and this was significantly blocked by cytochalasin D ($P = 0.0039$ and $P = 0.0041$, respectively). To confirm that cytochalasin D did not have a nonspecific effect on antigen presentation, we infected ALDC with rMVA-Ag85A at an MOI of 3 in the presence of cytochalasin D, fillipin, DMSO, and PBS and measured T cell activation by ELISPOT assay. All four treatments showed similar IFN-γ responses (data not shown).

MVA infection of ALDC downregulates costimulatory molecules in noninfected cells. The magnitudes of IFN-γ responses to Ag85A in experiments where ALDC were infected with rMVA (Fig. 1 and 4A) and in experiments where autologous noninfected ALDC were added to cells already infected with rMVA (Fig. 7B) were similar ($P = 0.1580$). To investigate why these responses were still low compared to responses obtained using rAd5-Ag85A, we infected 1×10^6 ALDC with a suboptimal concentration of rMVA-Ag85A (0.5 PFU/cell) for 60 min and washed them extensively to remove excess virus. We then added the same number of uninfected autologous ALDC. After an overnight culture, we measured cell death by PI incorporation and cell surface expression of CD40, CD80, CD86, MHC class I, and MHC class II by flow cytometry. Figure 8 shows the numbers and mean fluorescence intensities (MFI) of these molecules in mock-infected cells (Fig. 8A, D, G, J, and M). CD40, CD80, CD86, and MHC-II were downregulated in PI^+ ALDC, but interestingly, these were also downregulated in PI^- ALDC (Fig. 8B, E, H, and N). MHC class I was not downregulated in PI^+ ALDC, but in 5% of PI^- ALDC, this was downregulated (Fig. 8K). Antibody isotype controls were used to demonstrate that these were not binding nonspecifically to PI^+ cells (Fig. 8C, F, I, L, and O). To confirm that there was no residual virus in the system that could account for the observed effects on bystander cells, we infected ALDC with rMVA-GFP and washed them extensively as described above. Cells were then cocultured along with CEF, and GFP expression was assessed 16 h later by flow cytometry. Figure 8P shows that after the washing steps most of the inoculum is removed and fewer than 0.80% of permissive CEF cells show GFP expression compared to the level for CEF directly infected with rMVA-GFP. These results were also confirmed by fluorescence microscopy (data not shown).

MVA-infected ALDC promote chemoattraction of noninfected ALDC and T cells. To identify whether MVA-infected ALDC secreted chemokines which attracted noninfected cells, which could then take up apoptosing cells for antigen presentation, we used a trans-well assay to measure migration of both DC and T cells toward supernatants of MVA-infected ALDC. Dendritic cell migration levels were significantly higher in those samples containing supernatants from cells infected for 24 h than in samples containing supernatants from cells infected for 4 h (Fig. 9A). Similarly, T cell migration toward supernatants from MVA-infected DC for 24 h was at a significantly higher level than migration toward supernatants from mock-infected ALDC but was not statistically significant in samples containing supernatants from DC infected for only 4 h (Fig. 9B). Interestingly, more than 95% of the migrating ALDC expressed SIRPα, and two-thirds of these were $CD1b^+$ $CD21^+$ (Fig. 9C and D and data not shown).

DISCUSSION

Recombinant modified vaccinia virus Ankara (rMVA) has been and is being used in clinical trials of novel vaccines to induce immunity against tuberculosis (54), HIV infection (3, 59), and influenza (44), to name but three examples, with promising results. rMVA has been reported to induce antigen-specific immunoglobulins and $CD8^+$ T cell responses in humans as well as other species (1, 8, 15, 23), and the predominant mechanism by which the recombinant protein is presented to B and T cells *in vivo* is thought to be cross-presentation (57). The main role of dendritic cells is the presentation of antigen to T cells, in particular priming of naïve T cells within the lymph node (60, 73). Most systems used to investigate DC-T cell interactions rely on the isolation of monocytes or macrophages from blood or tissues (such as spleen or bone marrow) (63, 71) followed by maturation with IL-4 and GM-CSF or the harvesting of tissues followed by isolation of resident DC. Dendritic cells in the epithelia are thought to take up antigen by pinocytosis, macropinocytosis, or receptor-mediated endocytosis (6, 40, 51). Peripheral dendritic cells then migrate via the afferent lymphatic ducts to the draining lymph nodes, losing

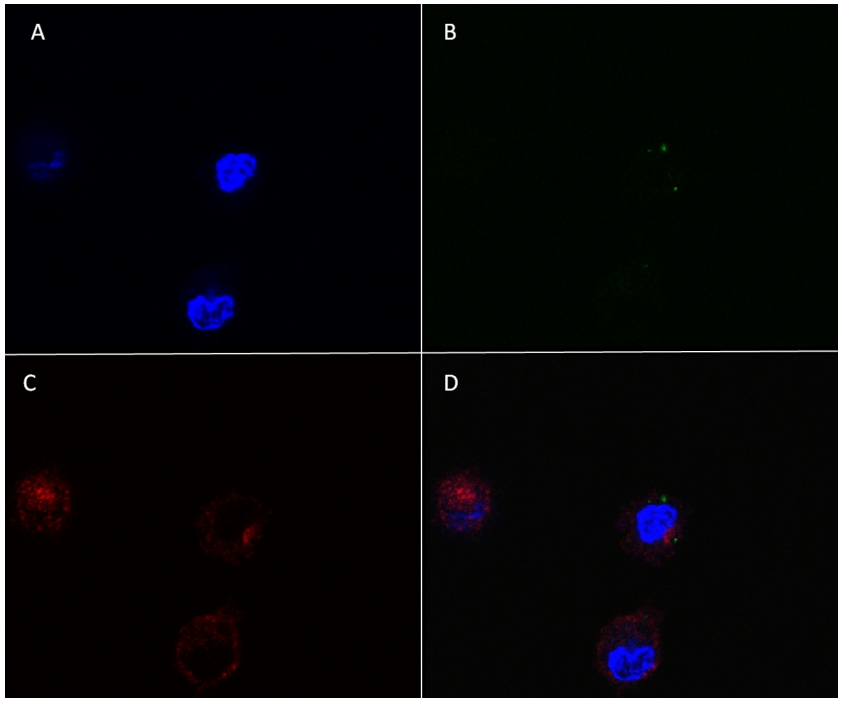

FIG 6 Apoptotic bodies from MVA-infected DC are taken up by noninfected ALDC. PKH-67-labeled ALDC (green) were infected with rMVA-Ag85A (MOI = 3) as described in Materials and Methods and cultured overnight at 37°C. Unlabeled autologous ALDC were added to the culture and incubated at 37°C for 4 h. Cells were stained, and FSC^{high} $MHCII^{+}$ $CD11c^{+}$ $DEC\text{-}205^{+}$ live single events positive for PKH-67 were FACS sorted, washed twice, mounted on a coverslip, and analyzed by confocal microscopy. Panel A shows DAPI; panel B shows PKH-67-labeled apoptotic bodies; panel C red shows DEC-205; panel D shows a merge of all three.

their ability to take up antigen but becoming very potent antigen-presenting cells. This model is challenged by the identification of dendritic cells from afferent lymph; these afferent lymph-veiled cells (51), which migrate from peripheral tissues, are able to process antigen and are potent stimulators of resting and naïve T cells.

We have previously shown that dendritic cells draining from the skin and collected by cannulation of pseudoafferent lymphatic vessels (34) are FSC^{high} $DEC\text{-}205^{+}$ $CD11c^{+}$ $CD8^{-}$ cells. Within this population, two major subpopulations can be identified, those cells expressing high levels of SIRPα and those expressing low levels or no detectable SIRPα (40, 51). Langerhans cells represent about 5% of the total number of migrating lymphatic DC, and all of these express SIRPα (33). Although both populations express high levels of costimulatory molecules (CD40, CD80, and CD86) and MHC class II, it is evident that only the $SIRP\alpha^{+}$ cells present antigen efficiently (40).

Tuberculosis is an infectious disease caused by *Mycobacteria* spp. in both humans and cattle, with important health and economic consequences. The use of heterologous prime-boost strategies has led to the development of recombinant vaccines to improve immunogenicity in humans and animals, and rMVA expressing the mycobacterial antigen 85A is a promising candidate for boosting T cell responses following priming with BCG (77, 83). We have recently described that dendritic cells draining from the skin and expressing SIRPα are efficiently targeted by recombinant vectors (17) and that rMVA induces apoptosis and cell death. We now describe the kinetics and mechanism of rMVA-induced apoptosis in DC draining from the skin. Our model is relevant in two ways: first, we are using dendritic cells draining from the skin with minimal manipulation, and so these are relevant in intramuscular/intradermal/subcutaneous vaccination protocols; second, we are using an animal model relevant to the disease since cattle are a host species for mycobacterial infection. While performing pilot experiments, we found that of the cells present in the afferent lymph, only DC were targeted by rMVA-GFP. In contrast, primary bovine skin fibroblasts showed >10% infection when an MOI of 100 PFU/cell of rMVA-GFP was used (data not shown), suggesting that DC are the primary infection target upon MVA injection. However, these data need to be confirmed *in vivo*. It is clear that even at low MOI, ALDC infected with rMVA are less efficient at presenting Ag85A compared to ALDC transduced with rAd5-Ag85A or pulsed with recombinant Ag85A protein (Fig. 1). Our data suggest that this is due to a very rapid induction of apoptosis (Fig. 2), evident in as little as 2 h postinfection, which prevents efficient rAg85A expression in the MVA-infected cells. Furthermore, MHC class I and II levels on the cell surface are concomitantly reduced. Although MVA-induced apoptosis has been described before in various DC cell models (2, 11, 43, 47), to our knowledge this is the first report showing the interaction of DC draining from the skin and MVA. Our data show that MVA-induced apoptosis occurs much faster than previously thought; this may be biologically important and highlights the need to use cells from anatomically relevant sites to understand the generation of immune responses.

We also show that MVA induces apoptosis via two caspase pathways, the extrinsic pathway characterized by the activation of caspase 8 and the intrinsic pathway characterized by the activation of caspase 9. In a model using human monocyte-derived DC,

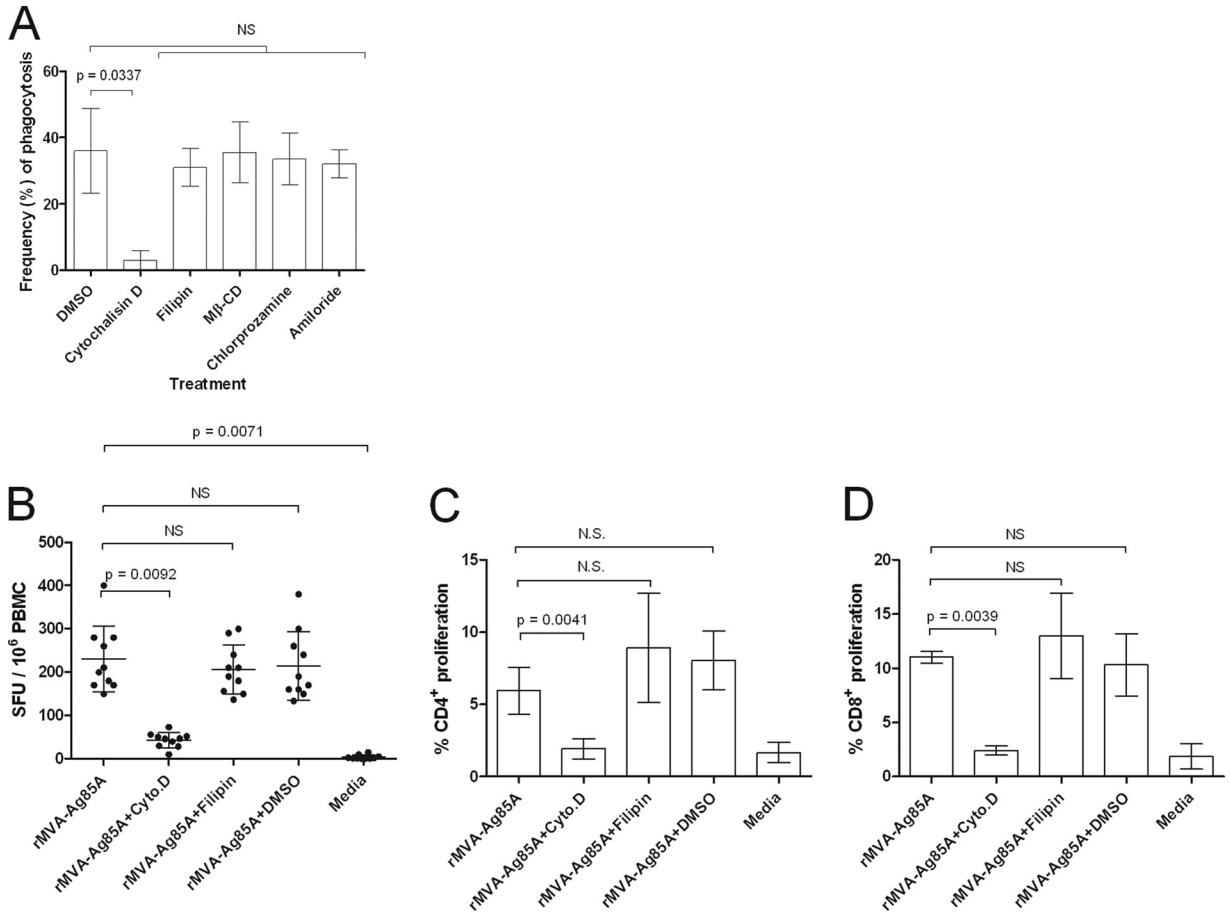

FIG 7 Uptake of apoptotic bodies by ALDC is by actin-mediated phagocytosis. (A) PKH-67-labeled ALDC were infected with rMVA-Ag85A (MOI = 3) as described in Materials and Methods. PKH-46-labeled autologous ALDC were added to the culture, incubated at 37°C for 4 h in the presence of the indicated inhibitors, and analyzed by flow cytometry. Cells were gated on FSC^{high} $MHCII^+$ $CD11c^+$ $DEC\text{-}205^+$ live single events. Bars represent means ($n = 10$) of results from events present in the upper right (UR) quadrant as shown in Fig. 5 (double positive for PKH-67 and PKH-46). Error bars indicate standard deviations. (B, C, and D) ALDC were infected with rMVA-Ag85A (MOI = 3), and after an overnight culture, autologous ALDC were added. Antigen presentation was measured by ELISPOT assay (B) or T cell proliferation by flow cytometry (C and D). Bars represent means of results from 10 animals analyzed in duplicate, and error bars indicate standard deviations. NS, not significant.

Brandler and colleagues showed that UV-inactivated rMVA-HIV did not induce apoptosis (4). However, here we show that caspase 8 is activated following virus binding or entry, demonstrated by the increase in caspase 8 activity in ALDC cultured with UV-inactivated MVA, initiating the caspase cascade. This suggests that an MVA-expressed pathogen-associated molecular pattern (PAMP) is responsible for the initiation of the extrinsic caspase pathway. Following virus entry and after 4 h postinfection, the caspase 9 cascade is initiated, promoting the expression of annexin V on the cell surface (Fig. 3), and both of these pathways can be blocked independently using caspase-specific inhibitors. We hypothesized that by blocking MVA-induced apoptosis, the antigen presentation capabilities of the rMVA-infected DC would improve. We showed increased antigen presentation to both $CD4^+$ and $CD8^+$ T cells, demonstrated by increased IFN-γ production and greater Ag85A-specific proliferation in samples containing caspase inhibitors compared to the levels in samples containing rMVA-Ag85A alone (Fig. 4). This suggests that under these conditions, direct presentation is responsible for T cell activation. Poxviruses are known to encode several apoptosis-inhibiting gene products (18, 22, 30, 42, 82), but the activity of these proteins in mammalian DC systems and their effect on recombinant poxvirus vaccination strategies are yet to be shown. Furthermore, many of these proteins are missing in the attenuated MVA strain (25). We are currently investigating vaccination efficacy and potency of recombinant MVA mutants that have a delayed capacity to induce apoptosis.

Because the magnitudes of IFN-γ responses to Ag85A in experiments where ALDC were infected with rMVA and in experiments where autologous noninfected ALDC were added to cells already infected with rMVA were not significantly different, we analyzed the levels of MHC class I, MHC class II, and costimulatory molecules in infected and cocultured noninfected DC. We have previously shown that *ex vivo* ALDC express high levels of these molecules and that they are downregulated following infection with rMVA (17). It is unclear how this downregulation occurs, but our experiments indicate that the expression of early viral proteins is required prior to the observed downregulation. We are currently investigating the effects of MVA protein expression on the surface expression of MHC and costimulatory molecules on ALDC. Here,

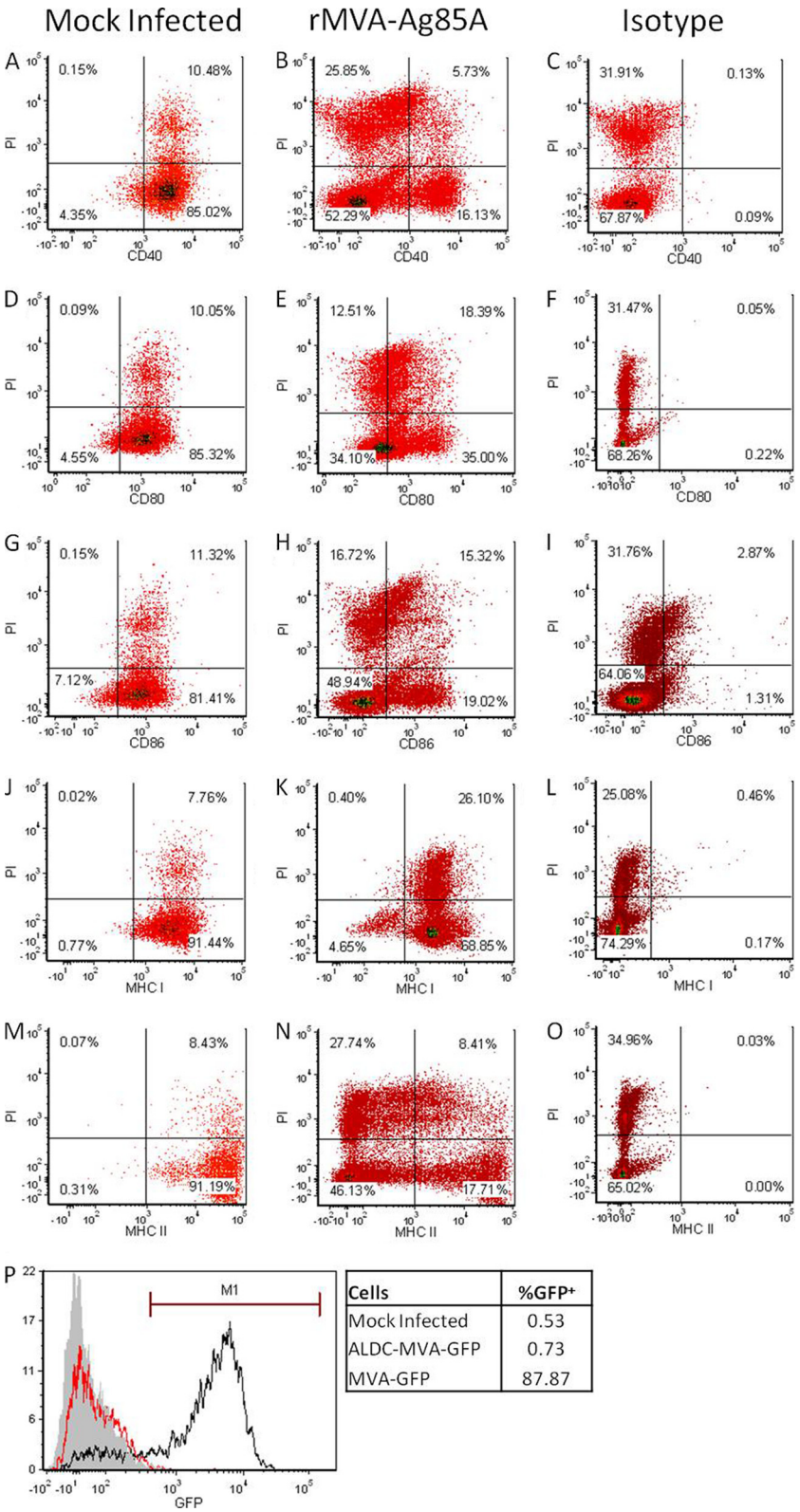

FIG 8 Infection by MVA downregulates expression of costimulatory molecules, MHC-I, and MHC-II in both infected and noninfected ALDC. ALDC (1×10^6) were mock infected (A, D, G, J, and M) or infected with rMVA-Ag85A (B, C, E, F, H, I, K, L, N, and O) using a suboptimal MOI of 0.5 PFU/cell at 4°C for 60 min to allow virus attachment; excess virus was removed by extensive washing, and the same number of uninfected autologous ALDC were added. After a 16-h culture at 37°C, the cells were harvested and stained with propidium iodide and mouse anti-bovine MAbs or isotype control antibodies and cell surface expression was analyzed by flow cytometry. Events shown were gated on single FSC^{high} DEC-205^+ events. Dot plots are representative of 3 independent experiments. (P) ALDC were mock infected (gray histogram) or infected (red histogram) with rMVA-GFP and washed as described above. Cells were then cocultured with chicken embryo fibroblasts (CEF) for 16 h at 37°C. Cells were then harvested, and GFP expression was measured by flow cytometry. The black histograms represent CEF infected with rMVA-GFP (MOI = 1). The overlay is representative of 3 independent experiments.

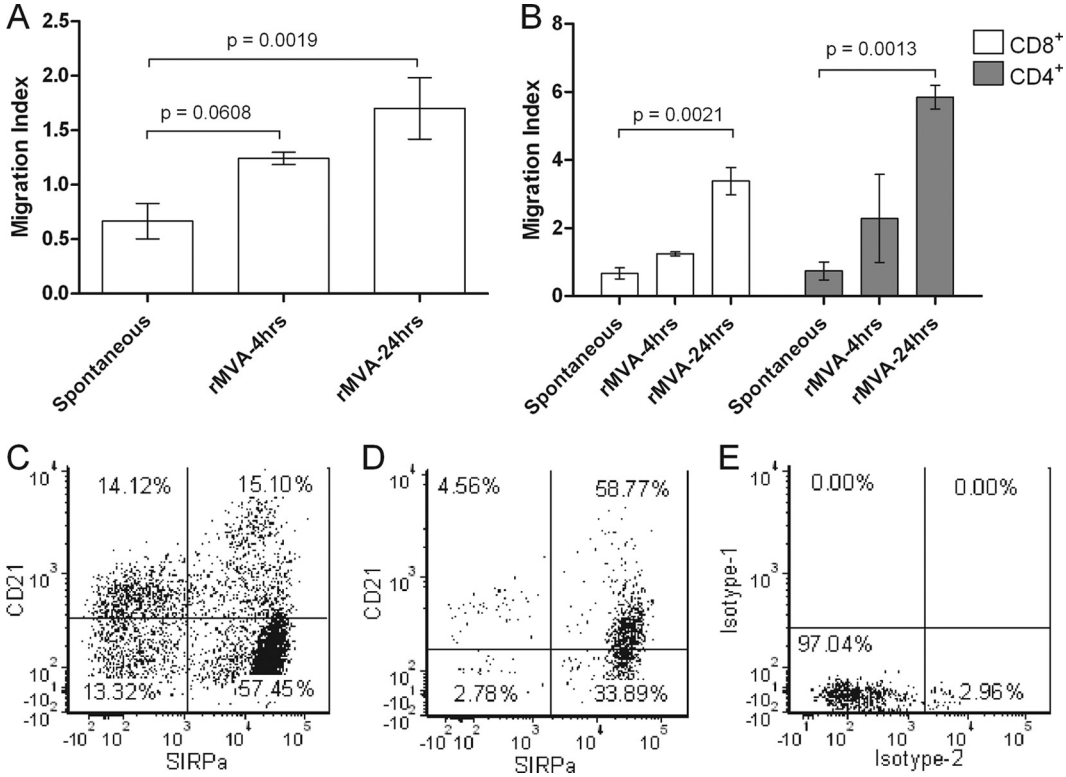

FIG 9 MVA-infected ALDC promote chemotaxis of noninfected DC and T cells. Tissue culture supernatants from mock-infected or MVA-infected ALDC (4 or 24 h of infection) were plated in triplicate onto the lower chamber of a trans-well assay plate. FACS-sorted ALDC (1×10^5) ($n = 6$) or T cells ($n = 5$) were then plated onto the upper chamber of the trans-well assay plate and incubated for 4 h at 37°C. Migration to the lower chamber was measured by flow cytometry. (A) Dendritic cell migration. (B) T cell migration. (C) Steady-state staining of ALDC showing expression of SIRPα and CD21. (D) Dot plot showing the phenotype of migrated DC. (E) Isotype controls. Dot plots are representative of 6 independent experiments performed in triplicate.

we confirm these results, but we also found that noninfected, PI^- ALDC showed downregulation of these molecules (Fig. 8). The downregulation of CD40 and CD86 was striking; in the case of MHC-II, the number of MHC-II^+ cells was reduced from >99% to <30% (Fig. 8M and N). Interestingly, MHC class I was not downregulated in PI^+ ALDC, but in 4% of PI^- ALDC, this was downregulated (Fig. 8K). The discrepancy between downregulation of MHC-I and that of MHC-II may provide an indication of why recombinant MVA induces stronger $CD8^+$ than $CD4^+$ T cell responses (4, 67) (Fig. 4 and 7). These data may also indicate why when poxvirus vectors are used levels of T cell response are generally lower than in vaccination strategies that utilize replication-deficient adenovirus vectors (9, 27, 61, 62, 77). At this moment, it is not known how MVA-infected ALDC affect surface receptor expression of bystander cells, but our preliminary data indicate that one or more soluble factors are involved in this phenomenon.

We then hypothesized that although DC were being killed by the rMVA, this prompted the generation of chemoattractants promoting migration of noninfected DC toward rMVA-infected DC. We show that supernatants from rMVA-infected DC promote migration of noninfected DC and also of T cells and that this activity is increased in supernatants from DC infected in the presence of caspase inhibitors (Fig. 9). Interestingly, most DC that migrated in our trans-well system were of the phenotype $SIRP\alpha^+$ $CD1b^+$ $CD21^+$. The biological importance of this is still unknown. ALDC have an average size of 20 to 30 μm, with some being as large as 45 μm, in diameter (our own observations); however, these are still capable of migrating across a membrane with pores of 5 or 8 μm in diameter. This demonstrates the plasticity and versatility of these cells. Following the migration of DC toward rMVA-infected DC, we show that the former cells take up cellular debris generated from the virus infection and subsequent cell death (Fig. 5 and 6). This cellular debris contains virus-expressed Ag85A, presumably in addition to other viral antigens. This phagocytosis requires actin (Fig. 7), and these subcellular fragments are processed for efficient presentation to $CD8^+$ and $CD4^+$ T cells (Fig. 7C and D). These data are supported by the recent publication of data showing that human peripheral blood monocytes take up antigens from MVA-infected leukocytes and thus promote DC maturation (24). Mouse and human DC models have been used to show that cross-priming is important in inducing T cell responses to recombinant antigens expressed by vaccinia vectors (26, 46, 69, 70). One important difference between the data presented here and other reports is that MVA-induced apoptosis is evident within a few hours of infection in DC draining from the skin but is not observed in *in vitro*-matured DC until much later (2, 11, 43). Another difference is that in mouse DC infected with MVA, the expression of costimulatory molecules such as CD40 and CD80 is reported to increase or remain unchanged (26), whereas we observe a fast downregulation of costimulatory molecules (17). This may be due to the origin of the DC studied and may be of physiological importance.

Our data indicate that following infection of ALDC with MVA, these cells secrete or release chemoattractants that induce migra-

tion of noninfected DC and T cells (Fig. 8). Although SIRPα-expressing DC represent about 70% of the total population of DC draining from the skin, only those expressing SIRPα migrated across the membrane toward supernatants from MVA-infected DC (Fig. 8D). Our laboratory is currently identifying the chemokines secreted by MVA-infected DC.

In the present study, we described a mechanistic view of antigen presentation and the generation of T cell responses to a recombinant antigen expressed by modified vaccinia virus Ankara. We have used the model of cannulation of pseudoafferent lymphatic vessels that drain from the skin to obtain dendritic cells relevant in intramuscular/intradermal/subcutaneous vaccination protocols. The biological material obtained requires minimal handling and does not require maturation *in vitro*, which may alter its biological functions, and thus provides a more accurate representation of DC interactions *in vivo*. However, here were only report the interaction of *ex vivo* cells with MVA *in vitro*, and so this interaction is investigated under steady-state conditions and optimized for the analysis ALDC. One important limitation of this system is the inability to account for inflammatory stimulus generated following the delivery of the vaccine through the skin using a needle, and the so the actual phenotype of cell infected *in vivo* and *in situ* is still unclear. We are currently addressing these limitations by vaccinating cannulated animals with MVA-GFP, as we have previously done for adenovirus vectors and the tuberculosis vaccine BCG (17, 33).

We provide evidence which indicates that MVA initiates DC apoptosis upon virus binding or entry via the caspase 8 pathway. Following virus entry, the caspase 9 pathway is activated and both pathways contribute to DC apoptosis. After MVA infection, DC begin to secrete or release chemokines or other cell-attracting molecules which are yet to be identified and induce migration of noninfected SIRPα$^+$ DC and T cells toward MVA-infected DC. Noninfected DC then take up apoptotic bodies and/or cellular debris and cross-present it to T cells, but there is still only modest induction of T cell responses. These studies suggest that modifying MVA vectors to reduce their capacity to induce apoptosis of dendritic cells is likely to result in enhanced T cell responses and so improve vaccine efficacy.

ACKNOWLEDGMENTS

We gratefully acknowledge the staff at IAH for care of cattle.

This work was funded by the Biotechnology and Biological Sciences Research Council, United Kingdom, and an industrial partnership award from Pfizer. J.C.H., S.C.G., and B.C. are Jenner Institute Investigators.

REFERENCES

1. **Antonis AF, et al.** 2007. Vaccination with recombinant modified vaccinia virus Ankara expressing bovine respiratory syncytial virus (bRSV) proteins protects calves against RSV challenge. Vaccine **25**:4818–4827.
2. **Behboudi S, Moore A, Gilbert SC, Nicoll CL, Hill AV.** 2004. Dendritic cells infected by recombinant modified vaccinia virus Ankara retain immunogenicity in vivo despite in vitro dysfunction. Vaccine **22**:4326–4331.
3. **Betts MR, et al.** 2005. Characterization of functional and phenotypic changes in anti-Gag vaccine-induced T cell responses and their role in protection after HIV-1 infection. Proc. Natl. Acad. Sci. U. S. A. **102**:4512–4517.
4. **Brandler S, et al.** 2010. Preclinical studies of a modified vaccinia virus Ankara-based HIV candidate vaccine: antigen presentation and antiviral effect. J. Virol. **84**:5314–5328.
5. **Brooke GP, Parsons KR, Howard CJ.** 1998. Cloning of two members of the SIRP alpha family of protein tyrosine phosphatase binding proteins in cattle that are expressed on monocytes and a subpopulation of dendritic cells and which mediate binding to CD4 T cells. Eur. J. Immunol. **28**:1–11.
6. **Butcher EC, Picker LJ.** 1996. Lymphocyte homing and homeostasis. Science **272**:60–66.
7. **Carroll MW, et al.** 1997. Highly attenuated modified vaccinia virus Ankara (MVA) as an effective recombinant vector: a murine tumor model. Vaccine **15**:387–394.
8. **Carson C, et al.** 2009. A prime/boost DNA/modified vaccinia virus Ankara vaccine expressing recombinant Leishmania DNA encoding TRYP is safe and immunogenic in outbred dogs, the reservoir of zoonotic visceral leishmaniasis. Vaccine **27**:1080–1086.
9. **Casimiro DR, et al.** 2003. Comparative immunogenicity in rhesus monkeys of DNA plasmid, recombinant vaccinia virus, and replication-defective adenovirus vectors expressing a human immunodeficiency virus type 1 gag gene. J. Virol. **77**:6305–6313.
10. **Cebere I, et al.** 2006. Phase I clinical trial safety of DNA- and modified virus Ankara-vectored human immunodeficiency virus type 1 (HIV-1) vaccines administered alone and in a prime-boost regime to healthy HIV-1-uninfected volunteers. Vaccine **24**:417–425.
11. **Chahroudi A, et al.** 2006. Differences and similarities in viral life cycle progression and host cell physiology after infection of human dendritic cells with modified vaccinia virus Ankara and vaccinia virus. J. Virol. **80**:8469–8481.
12. **Cheong C, et al.** 2010. Improved cellular and humoral immune responses in vivo following targeting of HIV Gag to dendritic cells within human anti-human DEC205 monoclonal antibody. Blood **116**:3828–3838.
13. **Colditz GA, et al.** 1994. Efficacy of BCG vaccine in the prevention of tuberculosis. Meta-analysis of the published literature. JAMA **271**:698–702.
14. **Contreras V, et al.** 2010. Existence of CD8alpha-like dendritic cells with a conserved functional specialization and a common molecular signature in distant mammalian species. J. Immunol. **185**:3313–3325.
15. **Coulibaly S, et al.** 2005. The nonreplicating smallpox candidate vaccines defective vaccinia Lister (dVV-L) and modified vaccinia Ankara (MVA) elicit robust long-term protection. Virology **341**:91–101.
16. **Crozat K, et al.** 2010. The XC chemokine receptor 1 is a conserved selective marker of mammalian cells homologous to mouse CD8alpha+ dendritic cells. J. Exp. Med. **207**:1283–1292.
17. **Cubillos-Zapata C, et al.** 2011. Differential effects of viral vectors on migratory afferent lymph dendritic cells in vitro predict enhanced immunogenicity in vivo. J. Virol. **85**:9385–9394.
18. **Dobbelstein M, Shenk T.** 1996. Protection against apoptosis by the vaccinia virus SPI-2 (B13R) gene product. J. Virol. **70**:6479–6485.
19. **Dorrell L, et al.** 2006. Expansion and diversification of virus-specific T cells following immunization of human immunodeficiency virus type 1 (HIV-1)-infected individuals with a recombinant modified vaccinia virus Ankara/HIV-1 Gag vaccine. J. Virol. **80**:4705–4716.
20. **Drexler I, Heller K, Wahren B, Erfle V, Sutter G.** 1998. Highly attenuated modified vaccinia virus Ankara replicates in baby hamster kidney cells, a potential host for virus propagation, but not in various human transformed and primary cells. J. Gen. Virol. **79**(Pt 2):347–352.
21. **Drillien R, Spehner D, Hanau D.** 2004. Modified vaccinia virus Ankara induces moderate activation of human dendritic cells. J. Gen. Virol. **85**:2167–2175.
22. **Eitz Ferrer P, et al.** 2011. Induction of Noxa-mediated apoptosis by modified vaccinia virus Ankara depends on viral recognition by cytosolic helicases, leading to IRF-3/IFN-beta-dependent induction of pro-apoptotic Noxa. PLoS Pathog. **7**:e1002083.
23. **Ferrer MF, et al.** 2011. Recombinant MVA expressing secreted glycoprotein D of BoHV-1 induces systemic and mucosal immunity in animal models. Viral Immunol. **24**:331–339.
24. **Flechsig C, et al.** 2011. Uptake of antigens from modified vaccinia Ankara virus-infected leukocytes enhances the immunostimulatory capacity of dendritic cells. Cytotherapy **13**:739–752.
25. **Garcia-Arriaza J, et al.** 2011. A candidate HIV/AIDS vaccine (MVA-B) lacking vaccinia virus gene C6L enhances memory HIV-1-specific T-cell responses. PLoS One **6**:e24244.
26. **Gasteiger G, Kastenmuller W, Ljapoci R, Sutter G, Drexler I.** 2007. Cross-priming of cytotoxic T cells dictates antigen requisites for modified vaccinia virus Ankara vector vaccines. J. Virol. **81**:11925–11936.
27. **Geiben-Lynn R, Greenland JR, Frimpong-Boateng K, Letvin NL.** 2008. Kinetics of recombinant adenovirus type 5, vaccinia virus, modified vaccinia ankara virus, and DNA antigen expression in vivo and the induction

of memory T-lymphocyte responses. Clin. Vaccine Immunol. **15**:691–696.
28. **Gliddon DR, Hope JC, Brooke GP, Howard CJ.** 2004. DEC-205 expression on migrating dendritic cells in afferent lymph. Immunology **111**:262–272.
29. **Gliddon DR, Howard CJ.** 2002. CD26 is expressed on a restricted subpopulation of dendritic cells in vivo. Eur. J. Immunol. **32**:1472–1481.
30. **Gubser C, et al.** 2007. A new inhibitor of apoptosis from vaccinia virus and eukaryotes. PLoS Pathog. **3**:e17.
31. **Guilliams M, et al.** 2010. From skin dendritic cells to a simplified classification of human and mouse dendritic cell subsets. Eur. J. Immunol. **40**:2089–2094.
32. **Hemati B, et al.** 2009. Bluetongue virus targets conventional dendritic cells in skin lymph. J. Virol. **83**:8789–8799.
33. **Hope JC, et al.** 2012. Migratory sub-populations of afferent lymphatic dendritic cells differ in their interactions with Mycobacterium bovis Bacille Calmette Guerin. Vaccine **30**:2357–2367.
34. **Hope JC, Howard CJ, Prentice H, Charleston B.** 2006. Isolation and purification of afferent lymph dendritic cells that drain the skin of cattle. Nat. Protoc. **1**:982–987.
35. **Hope JC, et al.** 2002. Development of detection methods for ruminant interleukin (IL)-12. J. Immunol. Methods **266**:117–126.
36. **Hope JC, et al.** 2005. Exposure to Mycobacterium avium induces low-level protection from Mycobacterium bovis infection but compromises diagnosis of disease in cattle. Clin. Exp. Immunol. **141**:432–439.
37. **Hope JC, et al.** 2005. Vaccination of neonatal calves with Mycobacterium bovis BCG induces protection against intranasal challenge with virulent M. bovis. Clin. Exp. Immunol. **139**:48–56.
38. **Howard CJ, et al.** 1991. Summary of workshop findings for leukocyte antigens of cattle. Vet. Immunol. Immunopathol. **27**:21–27.
39. **Howard CJ, Naessens J.** 1993. Summary of workshop findings for cattle (tables 1 and 2). Vet. Immunol. Immunopathol. **39**:25–47.
40. **Howard CJ, et al.** 1997. Identification of two distinct populations of dendritic cells in afferent lymph that vary in their ability to stimulate T cells. J. Immunol. **159**:5372–5382.
41. **Humrich JY, et al.** 2007. Vaccinia virus impairs directional migration and chemokine receptor switch of human dendritic cells. Eur. J. Immunol. **37**:954–965.
42. **Kalbacova M, Spisakova M, Liskova J, Melkova Z.** 2008. Lytic infection with vaccinia virus activates caspases in a Bcl-2-inhibitable manner. Virus Res. **135**:53–63.
43. **Kastenmuller W, et al.** 2006. Infection of human dendritic cells with recombinant vaccinia virus MVA reveals general persistence of viral early transcription but distinct maturation-dependent cytopathogenicity. Virology **350**:276–288.
44. **Kreijtz JH, et al.** 2009. Preclinical evaluation of a modified vaccinia virus Ankara (MVA)-based vaccine against influenza A/H5N1 viruses. Vaccine **27**:6296–6299.
45. **Kreijtz JH, et al.** 2009. Recombinant modified vaccinia virus Ankara expressing the hemagglutinin gene confers protection against homologous and heterologous H5N1 influenza virus infections in macaques. J. Infect. Dis. **199**:405–413.
46. **Larsson M, et al.** 2001. Efficiency of cross presentation of vaccinia virus-derived antigens by human dendritic cells. Eur. J. Immunol. **31**:3432–3442.
47. **Liu L, Chavan R, Feinberg MB.** 2008. Dendritic cells are preferentially targeted among hematolymphocytes by modified vaccinia virus Ankara and play a key role in the induction of virus-specific T cell responses in vivo. BMC Immunol. **9**:15.
48. **Liu Y, et al.** 2006. Hierarchy of alpha fetoprotein (AFP)-specific T cell responses in subjects with AFP-positive hepatocellular cancer. J. Immunol. **177**:712–721.
49. **Marquet F, et al.** 2011. Characterization of dendritic cells subpopulations in skin and afferent lymph in the swine model. PLoS One **6**:e16320.
50. **Mayr A, Stickl H, Muller HK, Danner K, Singer H.** 1978. The smallpox vaccination strain MVA: marker, genetic structure, experience gained with the parenteral vaccination and behavior in organisms with a debilitated defence mechanism. Zentralbl. Bakteriol. B **167**:375–390. (In German.)
51. **McKeever DJ, Awino E, Morrison WI.** 1992. Afferent lymph veiled cells prime CD4+ T cell responses in vivo. Eur. J. Immunol. **22**:3057–3061.
52. **McKeever DJ, MacHugh ND, Goddeeris BM, Awino E, Morrison WI.** 1991. Bovine afferent lymph veiled cells differ from blood monocytes in phenotype and accessory function. J. Immunol. **147**:3703–3709.
53. **McShane H, Behboudi S, Goonetilleke N, Brookes R, Hill AV.** 2002. Protective immunity against Mycobacterium tuberculosis induced by dendritic cells pulsed with both CD8(+)- and CD4(+)-T-cell epitopes from antigen 85A. Infect. Immun. **70**:1623–1626.
54. **McShane H, et al.** 2004. Recombinant modified vaccinia virus Ankara expressing antigen 85A boosts BCG-primed and naturally acquired antimycobacterial immunity in humans. Nat. Med. **10**:1240–1244.
55. **Meyer RG, et al.** 2005. A phase I vaccination study with tyrosinase in patients with stage II melanoma using recombinant modified vaccinia virus Ankara (MVA-hTyr). Cancer Immunol. Immunother. **54**:453–467.
56. **Moorthy VS, et al.** 2003. Safety and immunogenicity of DNA/modified vaccinia virus Ankara malaria vaccination in African adults. J. Infect. Dis. **188**:1239–1244.
57. **Norbury CC, et al.** 2004. CD8+ T cell cross-priming via transfer of proteasome substrates. Science **304**:1318–1321.
58. **Norder M, et al.** 2010. Modified vaccinia virus Ankara exerts potent immune modulatory activities in a murine model. PLoS One **5**:e11400.
59. **Ondondo BO, et al.** 2006. Immunisation with recombinant modified vaccinia virus Ankara expressing HIV-1 gag in HIV-1-infected subjects stimulates broad functional CD4+ T cell responses. Eur. J. Immunol. **36**:2585–2594.
60. **Palucka K, Banchereau J, Mellman I.** 2010. Designing vaccines based on biology of human dendritic cell subsets. Immunity **33**:464–478.
61. **Pillai VK, et al.** 2011. Different patterns of expansion, contraction and memory differentiation of HIV-1 Gag-specific CD8 T cells elicited by adenovirus type 5 and modified vaccinia Ankara vaccines. Vaccine **29**:5399–5406.
62. **Reyes-Sandoval A, et al.** 2010. Prime-boost immunization with adenoviral and modified vaccinia virus Ankara vectors enhances the durability and polyfunctionality of protective malaria CD8+ T-cell responses. Infect. Immun. **78**:145–153.
63. **Rossi M, Young JW.** 2005. Human dendritic cells: potent antigen-presenting cells at the crossroads of innate and adaptive immunity. J. Immunol. **175**:1373–1381.
64. **Rothberg KG, et al.** 1992. Caveolin, a protein component of caveolae membrane coats. Cell **68**:673–682.
65. **Sakr SW, et al.** 2001. The uptake and degradation of matrix-bound lipoproteins by macrophages require an intact actin cytoskeleton, Rho family GTPases, and myosin ATPase activity. J. Biol. Chem. **276**:37649–37658.
66. **Sallusto F, Cella M, Danieli C, Lanzavecchia A.** 1995. Dendritic cells use macropinocytosis and the mannose receptor to concentrate macromolecules in the major histocompatibility complex class II compartment: downregulation by cytokines and bacterial products. J. Exp. Med. **182**:389–400.
67. **Schafer B, et al.** 2011. Pre-clinical efficacy and safety of experimental vaccines based on non-replicating vaccinia vectors against yellow fever. PLoS One **6**:e24505.
68. **Schwartz-Cornil I, Epardaud M, Bonneau M.** 2006. Cervical duct cannulation in sheep for collection of afferent lymph dendritic cells from head tissues. Nat. Protoc. **1**:874–879.
69. **Serna A, Ramirez MC, Soukhanova A, Sigal LJ.** 2003. Cutting edge: efficient MHC class I cross-presentation during early vaccinia infection requires the transfer of proteasomal intermediates between antigen donor and presenting cells. J. Immunol. **171**:5668–5672.
70. **Shen X, Wong SB, Buck CB, Zhang J, Siliciano RF.** 2002. Direct priming and cross-priming contribute differentially to the induction of CD8+ CTL following exposure to vaccinia virus via different routes. J. Immunol. **169**:4222–4229.
71. **Steinman RM.** 1991. The dendritic cell system and its role in immunogenicity. Annu. Rev. Immunol. **9**:271–296.
72. **Stephens SA, Brownlie J, Charleston B, Howard CJ.** 2003. Differences in cytokine synthesis by the sub-populations of dendritic cells from afferent lymph. Immunology **110**:48–57.
73. **Streilein JW, Grammer SF, Yoshikawa T, Demidem A, Vermeer M.** 1990. Functional dichotomy between Langerhans cells that present antigen to naive and to memory/effector T lymphocytes. Immunol. Rev. **117**:159–183.
74. **Tsung K, Yim JH, Marti W, Buller RM, Norton JA.** 1996. Gene expression and cytopathic effect of vaccinia virus inactivated by psoralen and long-wave UV light. J. Virol. **70**:165–171.
75. **Vieth JA, Kim MK, Pan XQ, Schreiber AD, Worth RG.** 2010. Differen-

tial requirement of lipid rafts for FcgammaRIIA mediated effector activities. Cell. Immunol. **265**:111–119.
76. **Vordermeier HM, et al.** 2004. Cellular immune responses induced in cattle by heterologous prime-boost vaccination using recombinant viruses and Bacille Calmette-Guerin. Immunology **112**:461–470.
77. **Vordermeier HM, et al.** 2009. Viral booster vaccines improve Mycobacterium bovis BCG-induced protection against bovine tuberculosis. Infect. Immun. **77**:3364–3373.
78. **Wang LH, Rothberg KG, Anderson RG.** 1993. Mis-assembly of clathrin lattices on endosomes reveals a regulatory switch for coated pit formation. J. Cell Biol. **123**:1107–1117.
79. **West MA, Bretscher MS, Watts C.** 1989. Distinct endocytotic pathways in epidermal growth factor-stimulated human carcinoma A431 cells. J. Cell Biol. **109**:2731–2739.
80. **Whelan AO, et al.** 2003. Modulation of the bovine delayed-type hypersensitivity responses to defined mycobacterial antigens by a synthetic bacterial lipopeptide. Infect. Immun. **71**:6420–6425.
81. **Yrlid U, Macpherson G.** 2003. Phenotype and function of rat dendritic cell subsets. APMIS **111**:756–765.
82. **Yu E, et al.** 2011. Structural determinants of caspase-9 inhibition by the vaccinia virus protein, F1L. J. Biol. Chem. **286**:30748–30758.
83. **Zhu X, Venkataprasad N, Ivanyi J, Vordermeier HM.** 1997. Vaccination with recombinant vaccinia viruses protects mice against Mycobacterium tuberculosis infection. Immunology **92**:6–9.